Comparative study of vibration analysis in rotary shafts between Rayleigh's and Dunkerley's methods

Karrar Baher *　　　**Qasim A. Atiyah ***
Imad A. Abdulsahib***
*, **, *** *Mechanical Engineering Department / University of Technology / Baghdad / Iraq*
*Email: me.19.20@grad.uotechnology.edu.iq
**Email: 20044@uotechnology.edu.iq
***Email: 20018@uotechnology.edu.iq

Abstract

The importance of vibrations in rotating rotors in engineering applications has been examined, as has the best approach to interpreting vibration data. The most extensively used analytical approaches for rotating shaft vibration analysis have been investigated. In this research, a detailed study was made of the Rayleigh and Dunkerley methods due to their importance in the special calculations to find the amplitude of vibrations in the rotation system. The multi-node method was used to calculate both Dunkerley's and Rayleigh's methods. An experimental platform was built to study the vibrations that occur in the rotating shafts, and the results were compared with theoretical calculations and with different distances of the bearings. It proved that there is very little error between the experimental and theoretical results. The vibration signal from the sensors was analyzed using the LABVIEW program. Rayleigh's method was compared to the exact method, and it was considered the most accurate method. It was found that it made very little difference, up to about 0.06%. As for the Dunkerley method, the difference between it and the proper method is about 4%, which is acceptable. Then a comparison was made between Rayleigh's and Dunkerley's methods, and it was found that Dunkerley's method is the most appropriate in the calculations.

Keywords: *Vibrations, Rotating-Bearing System, Rayleigh, Dunkerley, LABVIEW.*

1. Introduction

Rotordynamics is the study of the dynamics of rotating machines. Rotordynamics varies from structural vibration research because of gyroscopic moments, cross-coupled forces, and the possibility of whirling instability [1]. Many industrial applications, including onboard space vehicles, revolving machinery in electrical power plants, and power transmission gear trains, utilize rigid rotor systems aided by linear or nonlinear elastic bearings. In rotating systems vibration can cause inefficiency, malfunction, and even catastrophic failure. As a result, modeling and understanding their complex behavior has become a prominent study topic [2-4].

A rotor-bearing mechanism can show undesirable subcritical super-harmonic resonances when the rotor's spinning speed is a part of its natural frequency [5]. Vibration is a natural occurrence in rotating machinery, but it has the potential to reduce productivity [6, 7].

Thus, while investigating the work of machines in general (and rotating machines in particular), vibrations are a serious concern for designers, engineers, and researchers. As a consequence, the focus will be on studying vibrations, determining the most appropriate method of analysis, and

determining the values of critical frequencies arising from an imbalance in machines.

Mass imbalance is the most common cause of harmonic excitation in rotating machinery. An

imbalance can arise during the assembling of machine components or during the manufacturing process of machine components. Even if a rotor is adequately balanced when it first starts up, its stability will diminish over time. Another vibration response, such as vibration from a nearby unbalanced rotating machine, could be excited at the base of a spinning machine with its own mass imbalance oscillation [2]. One of the most common causes of machine vibration is the inertia of the machine's moving elements. In a reciprocating motion, several components move back and forth. Newton's laws require that a force is applied to accelerate the mass, as well as a response from the force to the machine's structure. Periodic deflections are perceived as vibrations because the forces are generally periodic [1].

Tiwari [8] proposed a well-conditioned recognition technique for simultaneous calculation of residual imbalances, bearing stiffness, and damping coefficients based on the rotor's clockwise and counter-clockwise reactions. Reddy and Srinivas [9] investigated the dynamic analysis of a rotor with base excitation. With time histories, phase diagrams, and frequency responses, the effect of base excitation frequency and amplitude on rotor dynamics is demonstrated. Wang et al. [10] focused on the imbalance reaction, and they proposed an algorithm for detecting residual imbalances in the rotor and bearings at the same time. The rotor was represented as a homogenous and continuous Rayleigh beam. Yang and colleagues [11] used a new sort of TVRBSE based on the formulation of absolute node coordinates and Rayleigh beam theory under an arbitrary Lagrange-Euler description to develop a dynamic model of a moving and axially rotating Rayleigh beam. Zhu and J. Chung [12] used the proposed dynamical model to investigate the vibration and stability of a rotating Rayleigh beam with axial motion. To completely consider the terms of rotating inertia, they used the Rayleigh ray theory. Farshbaf Zinati, R., et al. [13] analyzed the stabilization and nonlinear vibration of a simply supported axially moving Rayleigh viscoelastic beam fitted with intermediate nonlinear support. Aouadi, M. A., & Lakrad, F. [14] discussed the three-dimensional bending linear free vibrations of rotating Rayleigh beams. The destabilization of free vibrations was found to be dependent on the linearization method that was used. Faraji Muhairi, M, et al. [15] studied the effect of

angular velocity on the balance and vibration of a simply supported Rayleigh shaft. The distinctions between the Rayleigh and Euler-Bernoulli models are presented. The influence of the slenderness ratio on the instability threshold and natural frequencies is seen. Zhu and Chung [16] addressed the beam's dynamic behaviors and properties, as well as a novel rotating beam model that is currently being implemented. The spinning beam's dynamic behavior and vibration frequency were compared in action. While examining the spinning beam, the Rayleigh beam model was found to be more accurate than the Euler-Bernoulli beam model.

Tamrakar and Mittal [17] used an impact hammer test to determine the system's fundamental frequencies, then determined the speed at which whirling occurs in the system. They used Dunkerley's natural frequency approach to verify the experimental results. Levy [18] has created an iterative technology based on Dunkerley's method for delivering natural vibration frequencies to discrete systems at the same time. Low [19] validated a Dunkerley expression referring to a uniform beam holding several masses. When compared to the result associated with the original property equation, it is discovered that Dunkerley's expression can yield a good approximation in general. Due to the impossibility of conserving computational time, Low strongly advised the Dunkerley approach for beams transporting more than two masses at separate locations.

Rayleigh and Dunkerley's approaches for analyzing vibrations have been utilized in prior studies, but without specifying which is better in the study or expressing a clear comparison between them. For this reason, it is necessary to clarify the two ways and choose which is the most appropriate in mathematical calculations for studying spinning machines and determining their frequency values.

The amplitude of vibrations in rotational systems will be determined using the Rayleigh and Dunkerley methods in this paper. It will also rely on the multi-node approach to calculate each of the Dunkerley and Rayleigh methods, compare them to one another, then compare both ways to the precise method to determine which is more accurate and recommended to utilize.

2. Mathematical Analysis

The stator, which supports the bearing, is frequently assumed to be stiff when modeling a

rotor device. In real-world applications, however, the rotor is frequently included in a more flexible structure, such as the framework of an aero-engine, which adds more compliance to the system and theoretically affects the influence of bearing nonlinearities [3].

2.1 Rayleigh's Method

The Rayleigh method for estimating the system's natural frequencies will be presented in this study. The system will be continuous, and you will be able to utilize this method to estimate the fundamental natural frequency of continuous systems [20]. It is critical to conduct a modal analysis of the rotors to avoid resonance during operation. A dynamic study of the rotating-shaft system under operating conditions is also necessary to assess the dynamic properties of the rotating system. By seeing the shaft as a spinning beam model, the system was mathematically modeled [21, 22].
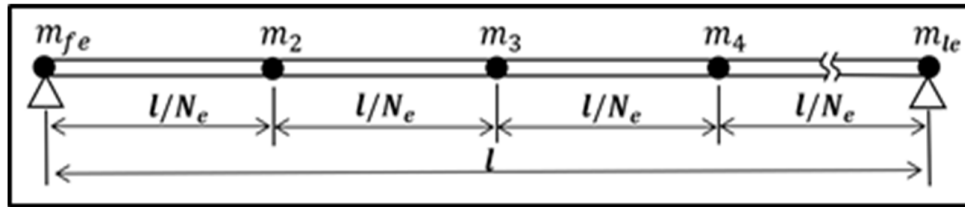

Fig. 1. Simply Supported Beam with finite nodes

The uniform beam for the number of nodes is shown in figure 1, and the masses for the nodes are computed using the following equations [23]:

$$m_{fe} = \rho V/2 = \frac{\rho A_{fe} L_{fe}}{2} \qquad \text{... (1)}$$

$$m_i = \frac{\rho A_i L_i}{2} + \frac{\rho A_{i+1} L_{i+1}}{2} \qquad \text{... (2)}$$

where $i = 1, 2, 3, \ldots, n$

$$m_{le} = \frac{\rho A_{le} L_{le}}{2} \qquad \text{... (3)}$$

The moment of inertia for the uniform solid beam is:

$$I_i = \frac{\pi}{64} * d^4 \qquad \text{... (4)}$$

It is possible to represent both the stiffness and the flexibility of a system's elastic behavior. The equations of motion for normal mode vibration in terms of stiffness K [23]:

$$(-\omega^2[M] + [K])\{y\} = 0 \qquad \text{... (5)}$$

In the stiffness conception, the force is expressed as a displacement:

$$\{F\} = [K]\{y\} \qquad \text{... (6)}$$

Stiffness is the polar opposite of flexibility. The displacement is given in units of force in this case:

$$\{y\} = [K]^{-1}\{F\} \qquad \text{... (7)}$$

$$\{y\} = [\delta]\{F\} \qquad \text{... (8)}$$

The $\delta_{i,j}$ coefficients of the flexibility matrix are

$$\begin{Bmatrix} y_1 \\ y_2 \\ \vdots \\ y_n \end{Bmatrix} = \begin{bmatrix} \delta_{11} & \delta_{12} & \cdots & \delta_{1n} \\ \delta_{21} & \delta_{22} & \cdots & \delta_{2n} \\ \vdots & & & \vdots \\ \delta_{n1} & \delta_{n2} & \cdots & \delta_{nn} \end{bmatrix} \begin{Bmatrix} f_1 \\ f_2 \\ \vdots \\ f_n \end{Bmatrix} \qquad \text{... (9)}$$

The flexibility influence coefficient $(\delta_{i,j})$ is the bending at i due to a unit load exerted at j with all other forces equal to zero. Deflections associated with $f_1 = 1$ and $f_2 = f_3 = 0$ are represented in the preceding matrix's first column. In the second column, you'll find deflections for $f_2 = 1$ and $f_1 = f_3 = 0$, and so on [23].

By multiplying Eq. 5 by $[K]^{-1} = [\delta]$, it is simple to determine the equation of motion in terms of flexibility:

$$(-\omega^2[\delta][M] + [I])\{y\} = 0 \qquad \text{... (10)}$$

Where,
$\{y\}$ is deflection vector matrix
$[m]$ is mass matrix
$[\delta]$ influence coefficient matrix equal $[k]^{-1}$
$[k]$ is stiffness matrix
$[I]$ is unit matrix, $K^{-1} * K$

$$\left| -\frac{1}{\omega^2} [I] + [\delta][m] \right| \qquad \text{... (11)}$$

When a lumped-mass system has a diagonal mass matrix, Eq. 11 becomes.

$$\left| -\frac{1}{\omega^2} \begin{bmatrix} 1 & 0 & \cdots & 0 \\ 0 & 1 & \cdots & 0 \\ \vdots & & & \vdots \\ 0 & 0 & \cdots & 1 \end{bmatrix} + \begin{bmatrix} \delta_{11} & \delta_{12} & \cdots & \delta_{1n} \\ \delta_{21} & \delta_{22} & \cdots & \delta_{2n} \\ \vdots & & & \vdots \\ \delta_{n1} & \delta_{n2} & \cdots & \delta_{nn} \end{bmatrix} \begin{bmatrix} m_1 & 0 & \cdots & 0 \\ 0 & m_2 & \cdots & 0 \\ \vdots & & & \vdots \\ 0 & 0 & \cdots & m_n \end{bmatrix} \right| = 0 \qquad \dots (12)$$
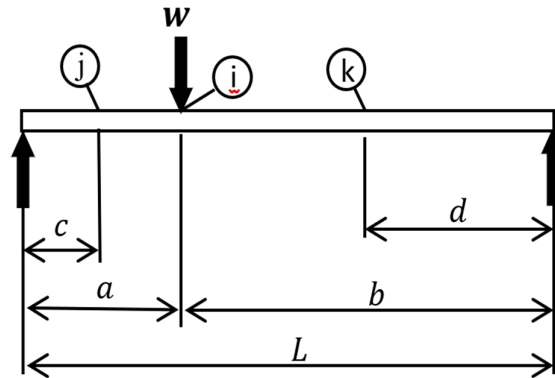

Fig. 2. Load exerted between the two bearings on a simply supported beam.

Figure 2 shows a simply supported beam with an applied load, from which the deflection equations for beams can be derived. The deflection will be as shown in Figure 2:

$$\delta_{ji} = w\mathrm{bc}(L^2 - b^2 - C^2)/6\mathrm{EIL} \qquad \dots (13)$$
$$\delta_{ii} = w\mathrm{a}^2 b^2/3\mathrm{EIL} \qquad \dots (14)$$
$$\delta_{ki} = w\mathrm{ad}(L^2 - a^2 - d^2)/6\mathrm{EIL} \qquad \dots (15)$$

Now the fundamental natural frequency of the beam is calculated based on equations 9 and 13 to 15.

$$\begin{aligned} y_1 &= F_1 * \delta_{11} + F_2 * \delta_{12} \\ &\quad + F_3 * \delta_{13} + \dots + F_n * \delta_{1n} \\ y_2 &= F_1 * \delta_{21} + F_2 * \delta_{22} \\ &\quad + F_3 * \delta_{23} + \dots + F_n * \delta_{2n} \\ y_n &= F_1 * \delta_{n1} + F_2 * \delta_{n2} \\ &\quad + F_3 * \delta_{n3} + \dots + F_n * \delta_{nn} \end{aligned}$$
$$\dots (16)$$

Where $F = m * g$.

The fundamental natural frequencies are obtained using equation 16 for a deflection given to several nodes in the simply supported beam.

Rayleigh's methods could be used to estimate the fundamental frequency of a beam or shaft defined by a series of lumped masses. The resulting constant deviation curve will be taken into account for weights $M_1 g, M_2 g, M_3 g, \dots$ which correspond to y_1, y_2, y_3, ... deviations. The stored energy in the beam due to strain is [21]

$$U_{max} = \frac{1}{2} g(M_1 y_1 + M_2 y_2 + M_3 y_3 + \cdots)$$
$$\dots (17)$$

$$K.E = \frac{1}{2}\omega^2(M_1 y_1^2 + M_2 y_2^2 + M_3 y_3^2 + \cdots)$$
$$\dots (18)$$
$$U_{max} = K.E \qquad \dots (19)$$
$$\omega^2 = \frac{g\sum M_i y_i}{\sum M_i y_i^2} \qquad \dots (20)$$

2.2 Dunkerley's Method

Dunkerley's method uses the natural frequencies of the constituent elements to derive the fundamental frequency of composite construction. It is acquired by leveraging the fact that the higher natural frequency bands of practically all vibrating systems are large in comparison to their fundamental frequencies. The frequency equation can be used to determine eigenvalues for a large system of degrees of freedom [20]:

The simplification procedures are done on equation 12, and then the formula is expanded to get the following formula:

$$\begin{aligned} \frac{1}{\omega_1^2} &+ \frac{1}{\omega_2^2} + \dots + \frac{1}{\omega_n^2} \\ &= \delta_{11} m_1 \\ &\quad + \delta_{22} m_2 + \dots + \delta_{nn} m_n \end{aligned}$$
$$\dots (21)$$

Because the intermediate frequencies ω_2, ω_3, ..., ω_n are often significantly larger than the fundamental frequency ω_1, and therefore

$$\frac{1}{\omega_i^2} \ll \frac{1}{\omega_1^2} \qquad i = 2,3,\ldots,n$$
$$\frac{1}{\omega_1^2} \approx \delta_{11}m_1 + \delta_{22}m_2 + \ldots + \delta_{nn}m_n$$
$$\ldots (22)$$

This equation is referred to as Dunkerley's formula. Eq. 22 produces a fundamental frequency that is never exactly the same as the exact number. In some cases, it would be easier to rewrite eq. 22 as:

$$\frac{1}{\omega_1^2} \approx \frac{1}{\omega_{1n}^2} + \frac{1}{\omega_{2n}^2} + \ldots + \frac{1}{\omega_{nn}^2} \qquad \ldots (23)$$

Where $\omega_{in} = (1 / \delta_{ii}m_i)^{1/2} = (k_{ii} / m_i)^{1/2}$ is the natural frequency of a single-degree-of-freedom system with mass m_i and a stiffness spring k_{ii}, $i = 1, 2, \ldots, n$. The lowest frequency of elasticity systems is calculated using Dunkerley's method.

3. Experimental Work

For this project, an experimental test platform was built to measure natural frequencies and take vibration readings. The main iron platform, which is a metal plate constructed of iron with dimensions of 120 cm x 40 cm x 5 mm that serves to carry the other parts was employed. A shaft is a spinning member that transmits rotational motion in the system. It is made of AISI 1045 steel and measures 80 cm in length and 20 mm in diameter. Two metal iron pieces, 40 cm long, 10 cm wide, and 10 mm thick were also used. The major role of these components is to support the pillow block bearing. In addition to being placed on the linear ball bearing block to modify the distances between the bearings, these pieces have a longitudinal groove

targeted at balancing devices and removing misalignments. There's also a linear sliding rail that holds the linear ball bearing block. Its job is to vary the distance between the bearings depending on where the measurements are to be made.

The system also has a ball bearing, (model UCP 204) made of cast iron with an inner diameter of 20 mm, a length of 124 mm, a thickness of 31 mm, a center height of 33.3 mm, and an overall height of 65 mm. A three-phase electric motor with a capacity of 0.37 kW and a maximum speed of 2825 rpm was also used. A coupling's main functions are to connect the shaft to the motor and reduce misalignment. It's also composed of iron, with a 43-mm outside diameter and a 98-mm length. The system also includes a power source for varying the motor's rotational speed, an Arduino UNO, and accelerometers mounted on a ball bearing to monitor the intensity of shaft vibrations, with measurements taken solely for the vertical axis. The details are shown in figures 3 and 4.

The vibration signal from the two accelerometers (mpu6050 and adxl335), with a variable rotational speed starting at 500 rpm and ending at 3000 rpm, was analyzed using the LABVIEW program. As indicated in figure 5, the sensors (mpu6050 and adxl335) were also employed for the calibration process between them. The readings from the LABVIEW program are in Hertz, and the system's frequency readings are taken on the Z vertical axis.
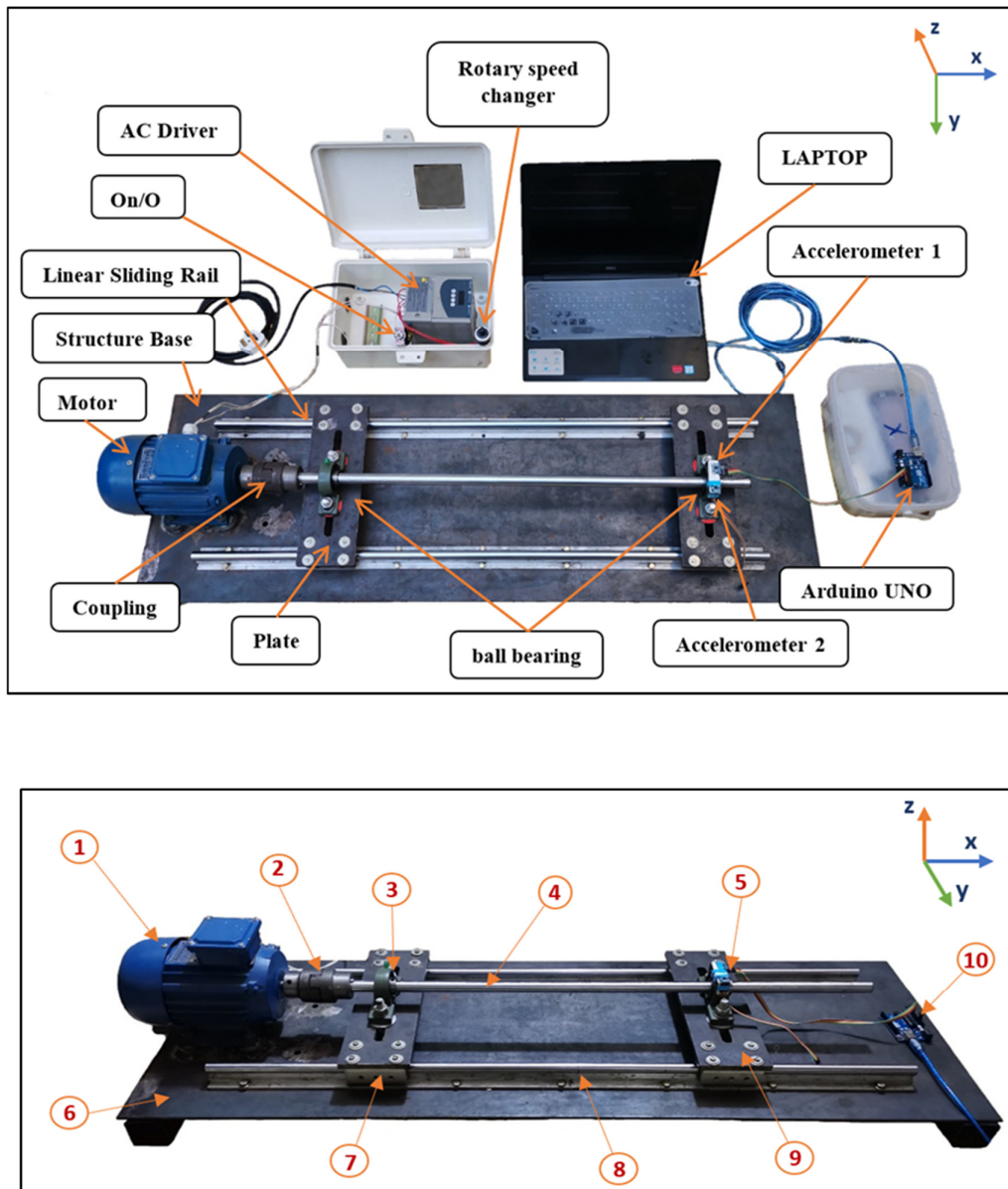
Fig. 4. The main components of the system.

The main components of the system in this work as shown in Figure 4:

1- Motor
2- Coupling
3- Ball bearing
4- Rotating shaft
5- Sensors

6- Main base
7- Linear Ball Bearing Block
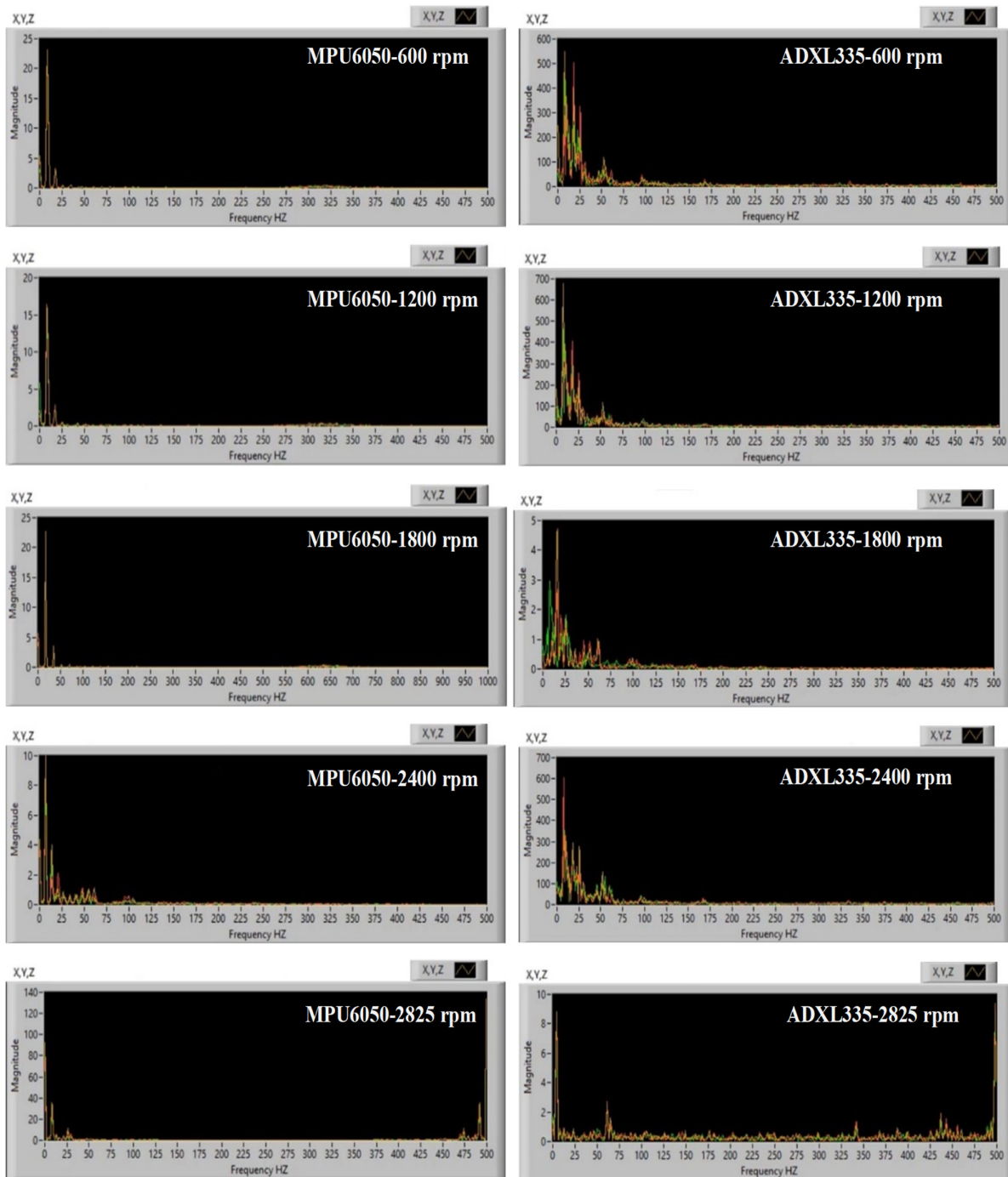8- Linear Sliding Rail
9- Iron pieces
10- Arduino UNO

Fig. 5. Calibration between MPU6050 and ADXL335.

4. Results and Discussion

The natural frequencies are derived using Dunkerley's approach from the critical frequency values that were retrieved using equation 22 and the results are compared with Rayleigh's uniform beam values, yielding the difference ratio between the two ways, as shown in Table 1. Given that Rayleigh's technique is more precise, it's worth noting that as the number of nodes employed for the uniform beam grows, the difference between the values reduces and the results converge. This suggests that the two procedures are in

agreement and that the results are accurate.

In practice, LabVIEW software will be used to find the frequency domain using mpu6050 and adxl335 sensors, with the two sensors being used to calibrate the results and note their reliability. The investigation was carried out in six distinct bearing positions.

The amplitude of rotating shaft vibrations at six distinct places along the vertical Z-axis was studied using the LabVIEW software in figures 7 to 12, and these positions are depicted in the simple schematic figure of Figure 6. When the distance between the bearings is lowered, it has been noticed that the values of the natural frequencies begin to fall. At around 65 Hz, the natural frequency reaches its maximum value, which is the first critical frequency of a spinning shaft in the first position. In the sixth position, it reaches its lowest critical frequency of 7 Hz. The values of the natural frequencies usually decrease as the distance between the bearings decreases, indicating that when the shaft becomes a hanging shaft, the value of the stresses is lower which reduces the size of the whirling along the shaft.

Table 1,
The frequencies of the uniform beam are calculated by using Rayleigh-Dunkerley's approach for a range of different nodes:

No. Nodes	Natural Frequency (Hz)		Difference %
	Rayleigh	Dunkerley	
5 - Nodes	62.52421	60.22316	3.68025
7 - Nodes	62.77290	60.50608	3.61116
9 - Nodes	62.56431	60.11276	3.91845
12 - Nodes	62.56956	60.10748	3.93496

The analytical approaches were investigated and compared to the exact method [20], with the Rayleigh method showing a difference of 0.0585 percent when compared to the exact method, and with the Dunkerley method showing a difference of 3.8788 percent when compared to the exact method.
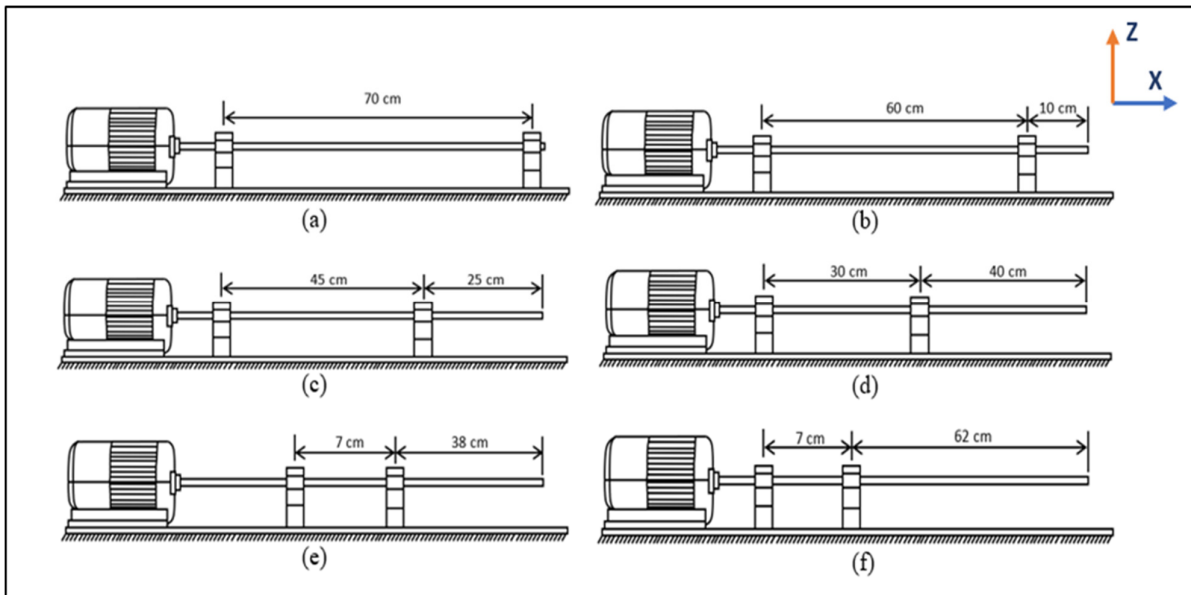
Fig. 6. Sketch between the bearings. (a) first position, (b) second position, (c) third position, (d) forth position, (e) fifth position, (f) sixth position.
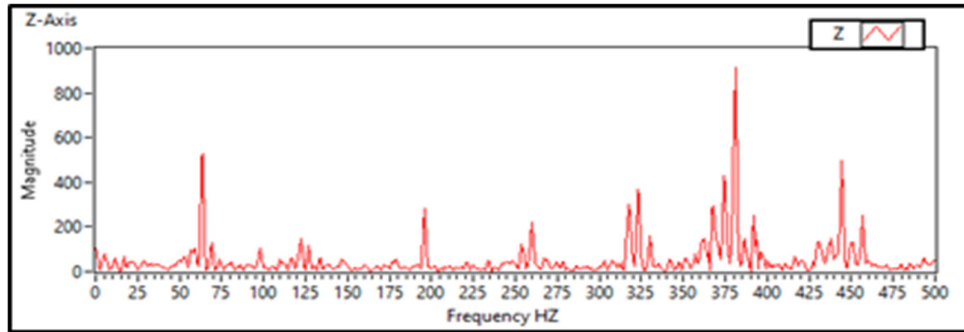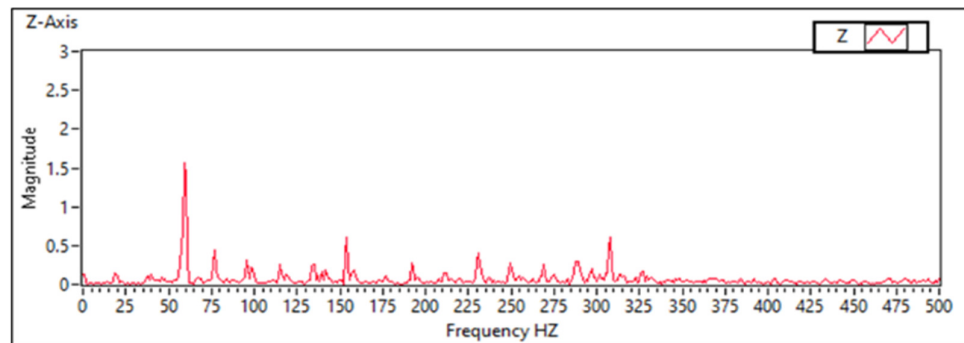
Fig. 7. Natural frequency of first position.

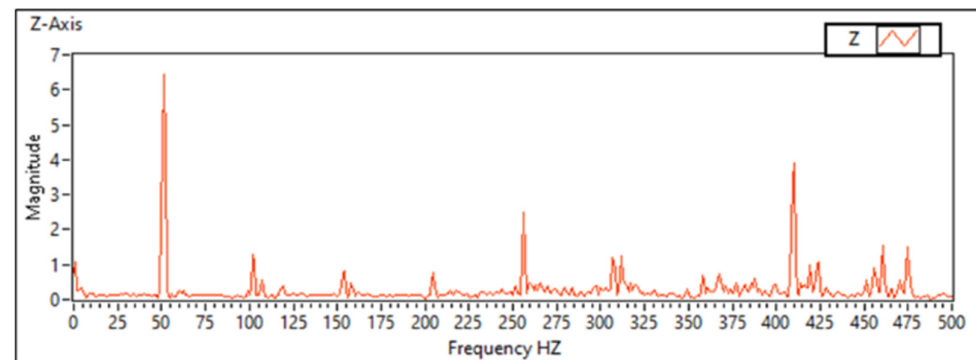

Fig. 8. Natural frequency of second position.

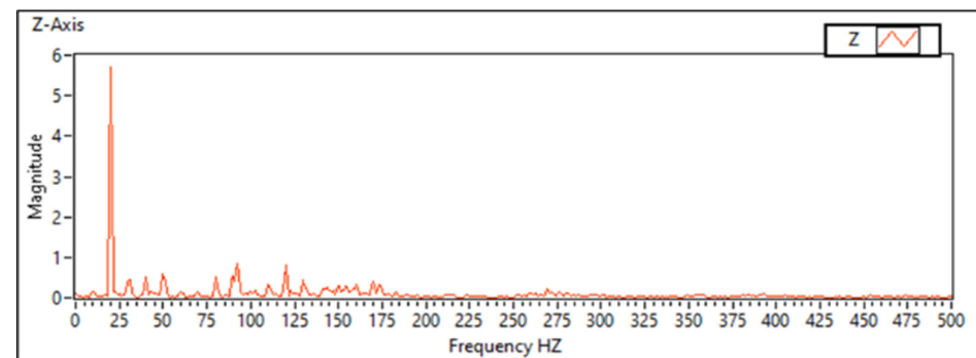**Fig. 9. Natural frequency of third position.**

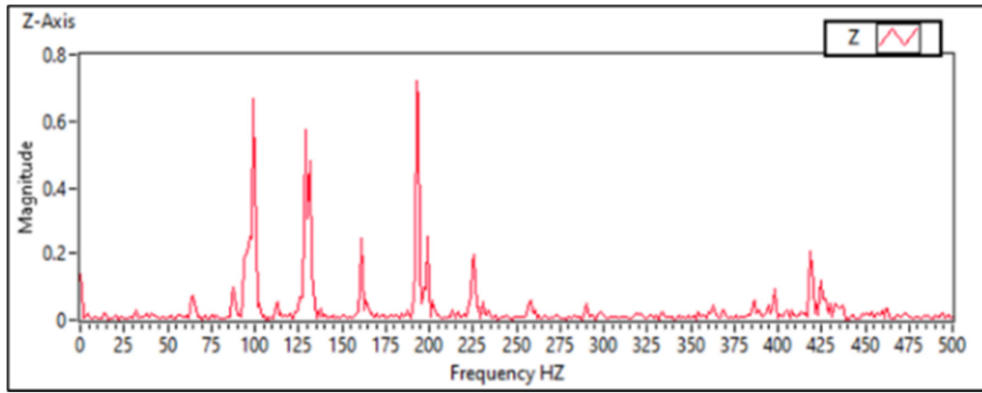**Fig. 10. Natural frequency of fourth position.**

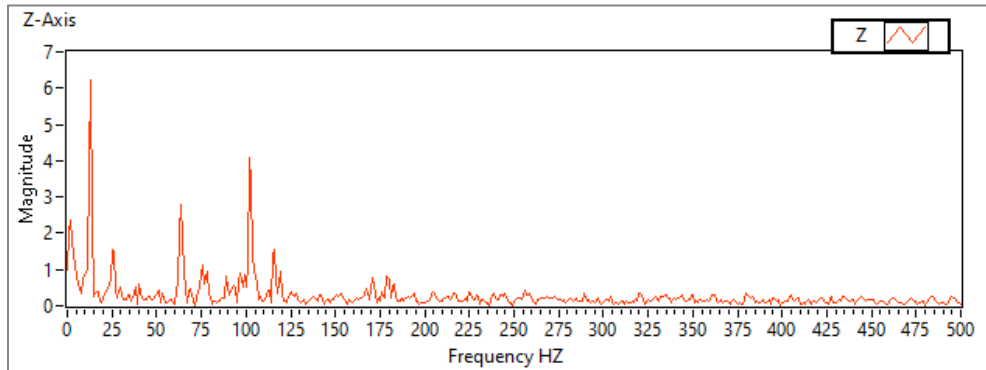**Fig. 11. Natural frequency of fifth position.**

Fig. 12. Natural frequency of sixth position.

In addition, a comparison was made between the experimental and numerical sides, and a percentage difference was discovered, which was close, as shown in Table 2.

Because real values exist on the experimental side and are more dependable in calculations and comparisons, there are values detected in the numerical and empirical aspects that are not found in the theoretical aspect that has been properly calculated.

Table 2,
Comparing the natural frequencies of the shaft numerically and experimentally.

No. of Position		1	2	3	4	5	6
1st Natural Frequency (Hz)	**Experimental**	65.013	59.548	50.835	20.134	5.536	5.235
	Numerical	60.762	67.235	60.933	22.651	6.6278	4.889
	Difference %	6.996	11.433	16.572	11.112	16.473	7.077
2nd Natural Frequency (Hz)	**Experimental**	125.845	155.435	105.735	93.648	100.153	35.686
	Numerical	141.88	141.88	99.612	111.11	118.38	35.656
	Difference %	11.301	9.553	6.146	15.715	15.397	12.325
3rd Natural Frequency (Hz)	**Experimental**	200.146	230.233	155.084	120.875	130.478	120.235
	Numerical	220.82	237.23	141.88	141.88	141.88	141.88
	Difference %	9.362	3.047	9.306	14.804	8.036	15.256

The first five natural frequencies were compared in table 3 between the numerical and experimental sides using ANSYS. The values

of the initial natural frequencies turn out to be close to a substantial extent, implying increased reliability.

Table 3,
Comparison of natural frequencies experimentally and numerically by ANSYS.

No. of Natural Frequency	Experimental (HZ)	Numerical (HZ)	Difference %
1st	65.013	60.762	6.99615
2nd	125.845	141.88	11.3018
3rd	200.246	220.82	9.31709
4th	380.856	389.94	2.32959
5th	440.218	420.77	4.622003

When the Rayleigh and Dunkerley methods were compared, it was discovered that the difference between them was relatively minor. For example, when using 7 nodes in the calculations for the two methods, the difference reached 3.6 percent, taking into account that the Rayleigh method is lengthy in the solution because it requires 25 flexibility values, whereas the Dunkerley method requires only 5 flexibility values. Bear in mind that the time at once is much less than the Rayleigh method. This saves effort in the calculations and is important in factories if productivity is important.

5. Conclusions

The Rayleigh and Dunkerley procedures for four states of nodes of a uniform shaft, which are used to determine the vibrations of rotating shafts, have all been thoroughly researched.
Through this study, the following conclusions were obtained:

1- By using a number of nodes to calculate the values of the natural frequencies of Rayleigh's and Dunkerley's methods, it was found that there is convergence in the results between the two methods, as the greater the number of nodes, the greater the accuracy and the more convergence in the results between the two methods.
2- The most suitable application method was determined to be the Dunkerley approach, which is close in results to the accurate method, with a little variation from the Rayleigh method of less than 4%.
3- The value of the natural frequencies reduces as the distance between the supporting bearings of the rotating shafts decreases. This result was tested and confirmed in six different positions for bearings.
4- When comparing experimental and numerical data, it was discovered that the difference in findings did not surpass 20 %. This indicates that the values were

converging and the results were accurate.
5- The amplitude of the vibrations generated in the system increases as the spinning shaft's speed increases. It can be shown that if the rotational speed is kept low, the system becomes more stable because the critical speeds are avoided.

List of Symbols

A_i	Cross sectional area at node i (m^2)
A_{fe}	Cross sectional area of first element (m^2)
A_{le}	Cross sectional area of last element (m^2)
d	Diameter (m)
E	Young's modulus (Pa)
F, f	Force (N)
$\{F\}$	Force vector matrix (N)
g	Gravitational acceleration (m / s^2)
I_i	Area moment of inertia for the uniform solid beam (m^4)
$[I]$	Unit matrix
K	Stiffness coefficient (N/m)
$[K]$	Stiffness matrix (N/m)
$K.E$	Maximum kinetic energy (J)
L_i	Length of element at node i (m)
L_{fe}	Length of first element (m)
L_{le}	Length of last element (m)
L	Length of shaft (m)
m_i	Ith mass of nodes (Kg)
m_{fe}	Mass of first node (Kg)
m_{le}	Mass of last node (Kg)
M, m	Mass (Kg)
$[M], [m]$	Mass matrix (Kg)
V	Volume (m^3)
U_{max}	Maximum potential energy (J)
w	Weight force applied to the beam (N)
ω	Natural frequency (rad/s)
y	Deflection of Beams (m)
$\{y\}$	Deflection of Beams vector matrix (m)
δ	Flexibility influence coefficient (m/N)
$[\delta]$	Influence coefficient matrix (m/N)
ρ	Mass density (kg / m^3)

6. References

[1] J. M. Vance, F. Y. Zeidan, and B. G. Murphy, *Machinery vibration and rotordynamics*. John Wiley & Sons, 2010.

[2] F. M. A. El-Saeidy and F. Sticher, "Dynamics of a Rigid Rotor Linear/Nonlinear Bearings System Subject to Rotating Unbalance and Base Excitations," Journal of Vibration and Control, vol. 16, no. 3, pp. 403-438, 2009, doi: 10.1177/1077546309103565.

[3] A. H. Haslam, C. W. Schwingshackl, and A. I. J. Rix, "A parametric study of an unbalanced Jeffcott rotor supported by a rolling-element bearing," Nonlinear Dynamics, vol. 99, no. 4, pp. 2571-2604, 2020, doi: 10.1007/s11071-020-05470-4.

[4] A. Khadersab and S. Shivakumar, "Vibration analysis techniques for rotating machinery and its effect on bearing faults," Procedia Manufacturing, vol. 20, pp. 247-252, 2018.

[5] J. Heikkinen, B. Ghalamchi, J. Sopanen, and A. Mikkola, "Twice-Running-Speed Resonances of a Paper Machine Tube Roll Supported by Spherical Roller Bearings: Analysis and Comparison With Experiments," in ASME 2014 International Design Engineering Technical Conferences and Computers and Information in Engineering Conference, 2014: American Society of Mechanical Engineers Digital Collection.

[6] R. V. Daniel, S. A. Siddhappa, S. B. Gajanan, S. V. Philip, and P. S. Paul, "Effect of Bearings on Vibration in Rotating Machinery," presented at the IOP Conference Series: Materials Science and Engineering, Karunya University, Coimbatore 641114, Tamil Nadu, India., 2017.

[7] G. Chandrashekar, W. Raj, C. Godwin, and P. S. Paul, "Study On The Influence Of Shaft Material On Vibration In Rotating Machinery," Materials Today: Proceedings, vol. 5, no. 5, pp. 12071-12076, 2018, doi: 10.1016/j.matpr.2018.02.182.

[8] R. Tiwari, "Conditioning of regression matrices for simultaneous estimation of the residual unbalance and bearing dynamic parameters," Mechanical Systems and Signal Processing, vol. 19, no. 5, pp. 1082-1095, 2005/09/01/ 2005, doi: https://doi.org/10.1016/j.ymssp.2004.09.005

[9] M. R. Reddy and J. Srinivas, "Vibration Analysis of a Support Excited Rotor System with Hydrodynamic Journal Bearings," Procedia Engineering, vol. 144, pp. 825-832, 2016, doi: 10.1016/j.proeng.2016.05.093.

[10] A. Wang, W. Yao, K. He, G. Meng, X. Cheng, and J. Yang, "Analytical modelling and numerical experiment for simultaneous identification of unbalance and rolling-bearing coefficients of the continuous single-disc and single-span rotor-bearing system with Rayleigh beam model," *Mechanical Systems and Signal Processing,* vol. 116, pp. 322-346, 2019, doi: 10.1016/j.ymssp.2018.06.039.

[11] S. Yang *et al.*, "Dynamic modeling and analysis of an axially moving and spinning Rayleigh beam based on a time-varying element," *Applied Mathematical Modelling,* vol. 95, pp. 409-434, 2021.

[12] K. Zhu and J. Chung, "Vibration and stability analysis of a simply-supported Rayleigh beam with spinning and axial motions," *Applied Mathematical Modelling,* vol. 66, pp. 362-382, 2019.

[13] R. Farshbaf Zinati, M. Rezaee, and S. Lotfan, "Nonlinear vibration and stability analysis of viscoelastic rayleigh beams axially moving on a flexible intermediate support," *Iranian Journal of Science and Technology, Transactions of Mechanical Engineering,* vol. 44, no. 4, pp. 865-879, 2020.

[14] M. A. Aouadi and F. Lakrad, "Linear flexural natural frequencies and stability analysis of spinning Rayleigh beams: application to clamped-clamped beams," in MATEC Web of Conferences, 2018, vol. 241: EDP Sciences, p. 01002.

[15] M. Faraji Mahyari, K. Faraji Mahyari, and S. Fardpour, "New Approach to Instability Threshold of a Simply Supported Rayleigh Shaft," *Journal of Solid Mechanics,* vol. 6, no. 2, pp. 150-157, 2014.

[16] K. Zhu and J. Chung, "Dynamic modeling and analysis of a spinning Rayleigh beam under deployment," *International Journal of Mechanical Sciences,* vol. 115-116, pp. 392-405, 2016, doi: 10.1016/j.ijmecsci.2016.07.029.

[17] R. Tamrakar and N. Mittal, "Experimental Investigation of Shaft Whirl Carrying 3 Rotors," *Trends in Mechanical Engineering & Technology,* vol. 5, no. 2, pp. 17-21, 2015.

[18] C. Levy, "An iterative technique based on the Dunkerley method for determining the natural frequencies of vibrating systems," *Journal of sound and vibration,* vol. 150, no. 1, pp. 111-118, 1991.

[19] K. Low, "A modified Dunkerley formula for eigenfrequencies of beams carrying concentrated masses," *International Journal of Mechanical Sciences,* vol. 42, no. 7, pp. 1287-1305, 2000.

[20] S. S. Rao, *Mechanical Vibrations in SI Units, Global Edition*, Sixth ed. Pearson, 2017.

[21] J. Metsebo, N. Upadhyay, P. Kankar, and B. N. Nbendjo, "Modelling of a rotor-ball bearings system using Timoshenko beam and effects of rotating shaft on their dynamics," *Journal of Mechanical Science and Technology*, vol. 30, no. 12, pp. 5339-5350, 2016.

[22] N. Wang, D. Jiang, and H. Xu, "Dynamic characteristics analysis of a dual-rotor system with inter-shaft bearing," *Proceedings of the Institution of Mechanical Engineers, Part G: Journal of Aerospace Engineering*, vol. 233, no. 3, pp. 1147-1158, 2019.

[23] W. T. Thomson, *Theory of vibration with applications*. CrC Press, 2018.

تحليل الاهتزازات في الأعمدة الدوارة باستخدام طريقتين رايلي ودونكرلي

كرار باهر تعيب*   قاسم عباس عطية**

عماد عبد الحسين عبد الصاحب***

*،**،***قسم هندسة الميكانيك/ الجامعة التكنولوجية/ بغداد/ العراق

*البريد الالكتروني: me.19.20@grad.uotechnology.edu.iq

**البريد الالكتروني: 20044@uotechnology.edu.iq

***البريد الالكتروني: 20018@uotechnology.edu.iq

الخلاصة

تم توضيح أهمية الاهتزازات للأعمدة الدوارة في التطبيقات الهندسية. تم اجراء دراسة على الطرق التحليلية الأكثر استخدامًا لتحليل الاهتزاز في عمود الدوران. حيث أنه في هذا البحث تم إجراء دراسة تفصيلية لطريقتي Dunkerley و Rayleigh نظراً لأهميتهما في الحسابات الرياضية لإيجاد سعة الاهتزازات في نظام الدوران. تم استخدام طريقة العقد المتعددة للحساب في كل من طريقة Dunkerley و Rayleigh. تم إنشاء منصة تجريبية لدراسة الاهتزازات التي تحدث في الأعمدة الدوارة ومقارنة النتائج مع الحسابات النظرية ولمسافات المختلفة بين المحامل. ثبت أن هناك توافق جيد بين النتائج التجريبية والنظرية. باستخدام برنامج LABVIEW تم تحليل إشارة الاهتزاز القادمة من المستشعرات. تمت مقارنة طريقة رايلي بالطريقة الدقيقة، وتم اعتبارها الطريقة الأكثر دقة. وقد وجد أنها تحدث فرقًا بسيطًا جدًا، يصل إلى حوالي ٠,٠٦٪. أما طريقة دنكرلي فالفرق بينها وبين طريقة الدقيقة يبلغ حوالي ٤٪ وهي مقبولة. ثم تم إجراء مقارنة بين طريقتين Rayleigh وDunkerley، ووجد أن طريقة Dunkerley هي الأنسب في الحسابات.